World Scientific
www.worldscientific.com

Adaptive preload controller design and analysis for electrostatic suspension system

Yukun Wang[*,§] and Zhi Wang[*,†,‡,¶]

[*]*Changchun Institute of Optics, Fine Mechanics and Physics,
CAS, Changchun 130033, P. R. China*

[†]*Taiji Laboratory for Gravitational Wave Universe (Beijing/Hangzhou),
University of Chinese Academy of Sciences (UCAS), Beijing 100049, P. R. China*

[‡]*School of Fundamental Physics and Mathematical Sciences,
Hangzhou Institute for Advanced Study, UCAS, Hangzhou 310024, P. R. China*

[§]*wangyukun@ciomp.ac.cn*
[¶]*wz070611@126.com*

[‖]*On behalf of The Taiji Scientific Collaboration*

The electrostatic suspension control system (ESCS) is the core component of the inertial sensor in space gravitational wave detection. To adapt to the changes in orbit environment and satellite platform vibration, the test mass stable is kept in the center of the electrode cage, the ESCS requires high-precision parameters calibration and high-stability verification of the control system. This paper studied the ESCS method, an adaptive controller with variable preload was proposed, and the stability conditions of the control system are given to provide a theoretical basis for the design of the controller. The structure and working principle of the system were also introduced. The electrostatic control system model was derived, and the performance of adaptive preload controller was analyzed. Finally, a simulation was conducted under different disturbance conditions. The results show that the control method proposed in this paper can achieve stable control in difference disturbance, and the preload voltage will change with the conditions. Compared with the traditional fixed preload method, we can see that our method has significantly improved the stability margin and the control quality during the process of dynamic response. This paper provides a solid foundation for the future exploration of space gravitational waves in China and clears the optimization direction for the next step.

Keywords: Gravitational wave detection; Chinese Taiji Program; inertial sensor; electrostatic suspension control system; adaptive preload control.

All authors contributed equally to this work.
[§,¶]Corresponding authors.
[‖]For more details, please refer to article 2102002 of this Special Issue.

1. Introduction

After the detection of gravitational wave by Laser Interferometer Gravitational Wave Observatory (LIGO) in February 2016, the prediction of Einstein regarding the existence of gravitational waves was confirmed.[1] From then on, a lot of Gravitational wave events have been discovered.[2–4] The detection of gravitational waves has epoch-making importance in the history of astronomy and physics, which officially opened the era of gravitational wave astronomy. Ground gravitational wave measurement is affected by the gravity of earth. The range of detected gravitational waves is mainly concentrated in the mid-high frequency of 10 Hz to 10 kHz. However, gravitational wave information is abundant in the low-frequency range of 0.1 mHz to 1 Hz. Space gravitational wave detection is the only option for studying gravitational waves in low-frequency range.

Space gravitational wave detection uses an ultra-high-precision interferometric measurement system to measure the distance change between the two test masses (TM) in inertial sensor (IS). The IS is one of the most important parts of space gravitational wave detection instrument. The main function of this sensor is to release the TM into space freely and realize drag-free control. Simultaneously, the electrostatic suspension control system (ESCS) is used to ensure the maximum movement of the TM along the geodesic, the performance of the ESCS directly affects the success or failure of space gravitational wave detection project.

Internationally, the United States and Europe have used the electrostatic suspension accelerometer to launch MESA, ASTRE, STAR, GRADIO, and other accelerometers, and the earliest project to develop space gravitational wave detection was the collaborative space laser interference antenna laser interferometer space antenna (LISA) project of NASA and the European Space Agency (ESA) in the 1990s.[5] In December 2015, the LISA pathfinder was launched to demonstrate and test LISA-related technology.[6] As a representative of space gravitational wave detection project, LISA has drawn a clear path and platform for space gravitational wave detection discipline at the level of the mission concept.

In China, the Huazhong University of Science and Technology,[7–9] the Lanzhou Institute of Physics[10,11] and the Changchun Institute of Optics Fine Mechanics and Physics[12] researched on electrostatic suspension accelerometers since 2000, and have space application such as Tianzhou-1 satellite, Taiji-1 satellite and Tianqin-1 satellite. Chinese scientists have conducted substantial research work with the support of the Strategic Priority Research Program of the Chinese Academy of Science. Scientific goals, development routes, program planning, and key technical breakthroughs were proposed, and the Space Taiji Program was introduced in early 2016.[13,14] According to the plan, China will launch a gravitational wave detection satellite group around 2030 to conduct direct detection of gravitational waves in the middle and low-frequency bands.

Numerous key technical tasks must be conducted because the technical indicators required for the Taiji Program are much higher than those of the current

state of technology. One of the most important tasks is the ESCS. When the ESCS works in space, the parameters of ESCS will change due to the influence of space environment and the switching of working mode. In addition, it will be affected by satellite vibration and overload shock. Many experts and scientists have focused on the research of control methods for ESCS, and various advanced control methods have been proposed[15–17] The most studied method is the PID and its modification. This is a linear time-invariant control method, and cannot solve the contradiction of rapidity and overshoot. For the nonlinearity and uncertainty of the actual ESCS, this method cannot fully meet the control requirement of stability, fast response and low overshoot response. In order to improve the stability and control ability, it is necessary to select a large preload voltage. However, it is desirable to select a small preload voltage to guarantee the noise level of the ESCS.

In order to solve this contradiction and meet the control requirements of the future Chinese space gravitational wave detection mission (Taiji Program), this paper performs the key technical research of the ESCS, an adaptive preload control (APC) scheme is proposed by accurately linearizing the system model and changing the preload voltage adaptively by the measured acceleration in real time. To verify our method, a simulation with different disturbance is conducted. The results show that the system performance is basically not affected by the change of preload voltage, the ESCS can work stable under different conditions. The stability and the control performance have been improved a lot compared with traditional fixed preload method. This study provides optimization direction and design ideas for future ESCS research.

The content of this paper is as follows. Section 2 mainly introduces the basic working principle and theoretical model derivation of the ESCS. Section 3 provides the design of APC. Section 4 conducts a simulation and the results are analyzed. Section 5 gives a comprehensive summary of the work in this paper.

2. Working Principle and Control System Model

2.1. *Working principle*

The IS comprises of two units: sensor and front end electronic (FEE). The sensor is used to sense the external interference acceleration signal and convert this signal into a differential capacitance displacement signal which will finally enter the FEE unit.

As is shown in Fig. 1, the sensor comprises of one TM and six pairs of electrodes, each pair of electrodes realizes one-degree of freedom for the ESCS. The TM and the surrounding electrode pair form a capacitance bridge, and the position of the TM is detected by differential capacitance. The six electrode pairs are X1, X2, X3, Y, Z1 and Z2. These electrode pairs can realize three translations and three rotations. Figure 2 shows the measurement principle.
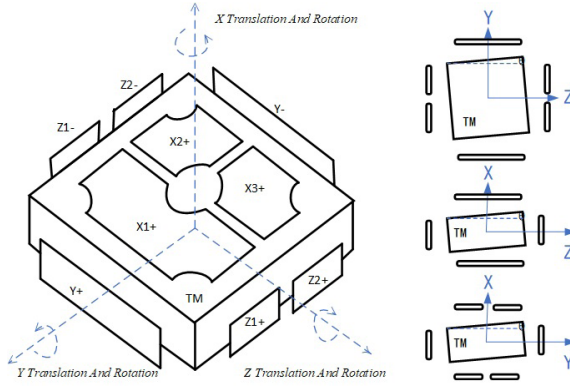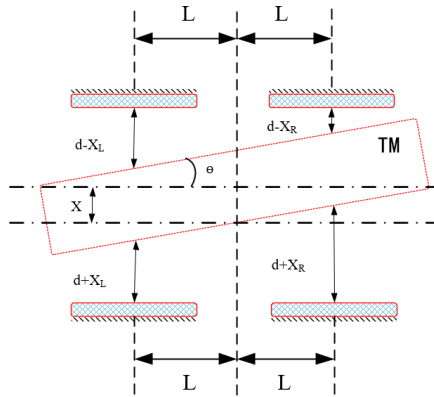
Fig. 1.   Woring principle of IS.

Fig. 2.   Measurements of translation and rotation.

As shown in Fig. 2, the translational displacement X and rotational angle θ can be calculated by the following equation:

$$\begin{cases} X = \dfrac{X_R + X_L}{2}, \\ \theta = \arctan\left(\dfrac{X_R - X_L}{2L}\right), \end{cases} \tag{1}$$

where X_L is the offset from the center of the left electrode pair, X_R is the offset from the center of the right electrode pair, L is the distance from the center of the electrode to the TM central axis and d is the average gap of the electrode pairs.

The FEE is mainly used to detect the differential capacitance signal from the sensor and send the corresponding servo feedback voltage signal to the electrode pairs. The electrostatic force is provided by the servo feedback voltage to keep the TM at the center of the structure and achieve linear measurement of the acceleration signal, the feedback voltage represents the acceleration signal. The purpose of ESCS

is to calculate the driving voltage by the capacitance displacement. The degrees of freedom are theoretically decoupled, however, there is a certain coupling between each degrees of freedom due to machining errors and assembly errors, which requires the control system to adapt to this coupling and make the ESCS work stably. The performance of the ESCS directly determines the stability and reliability of the IS.

The working principle is shown in Fig. 3. V_d is the injection voltage signal used for differential capacitance detection. V_p is the preload voltage for the electrostatic drive. V_d and V_p are applied to the TM through a gold wire. When an external interference force acts on the TM, the TM will deviate from the center of the electrode pairs. This phenomenon will result in a change in capacitance C_1 and C_2. C_1 is the capacitance between the TM and the upper electrode, while C_2 is the capacitance between the TM and the lower electrode. The differential capacitance signal C_1–C_2 is detected by the capacitive sensing circuit in FEE. After the signal demodulation and low-pass filter modules, the differential capacitance signal finally enters the control module. The feedback voltage signal V_f is then applied to the electrodes through the electrostatic drive circuit, V_f is calculated by the controller module, and the TM is pulled back to the center of the electrode pairs by the electrostatic force. This feedback voltage reflects the magnitude of the external interference acceleration.

When the TM is stably controlled at the center of the electrode pairs, the feedback voltage and the external interference acceleration satisfy the following relationship:[12]

$$a_e \cong \frac{2\varepsilon_0\varepsilon_r S}{md^2} V_p V_f, \tag{2}$$

where ε_0 is the vacuum dielectric constant, ε_r is the relative dielectric constant, S is the electrode area, d is the average gap between the electrode and the TM, V_f is the feedback control voltage and V_p is the preload voltage applied to the TM.
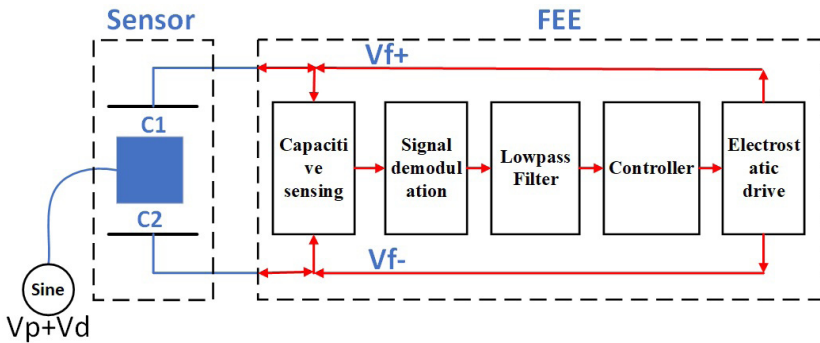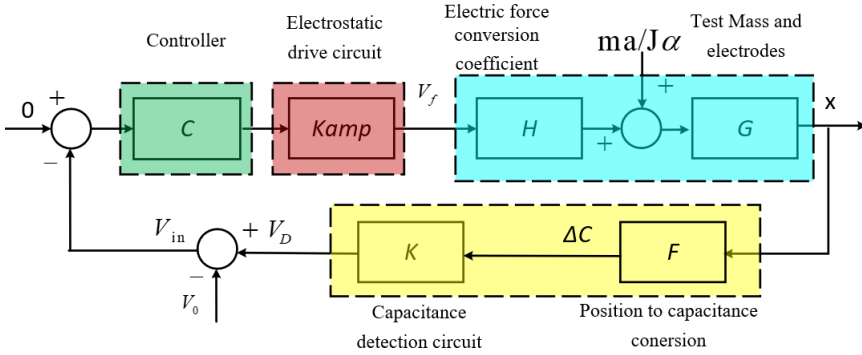

Fig. 3.   Working principle of IS.

Fig. 4.   Block diagram of ESCS.

2.2. *Control system model*

The ESCS is comprised of three parts: differential capacitance detection circuit, electrostatic driving circuit and electrostatic suspension controller. Figure 4 shows a block diagram of the closed-loop control system.

In Fig. 4, C in the green box is the digital controller. K_{amp} in the red box represents the gain of the electrostatic drive circuit, the module in the blue box is the kinetic model of electrostatic suspension system, H is the conversion coefficient from voltage to force, G is the electrostatic model, F is the conversion function from position to differential capacitance and K in the yellow box denotes the gain of the capacitive detection circuit. The above-mentioned modules linked together form a negative feedback closed-loop control system. Because of the bandwidth of the circuits is larger than the working frequency domain, these two modules can be considered as proportional K and K_{amp}. The design of the capacitance detection and electrostatic driving circuits is detailed in our precious work.[12]

In the ESCS, there are two modules in the entire system which are nonlinear when the TM is far from the center of electrode pairs. This nonlinear characteristics will lead to unstable of the system at the initial state or large disturbance situation, which is due to that the controller is designed under linear system model. Hence, it is important to analyze the nonlinear characteristics and linearize the system model.

The first nonlinear module is F in the yellow box. When there is a displacement x, the relationship between differential capacitance $\Delta C = C_1 - C_2$ and displacement x can be written as[17]

$$\Delta C = \frac{2\varepsilon_0 \varepsilon_r S}{d^2 - x^2} x. \tag{3}$$

After amplification by the capacitance detection circuit K times, the output voltage is V_D, then there is

$$V_D = F(x) = \Delta C K = \frac{2\varepsilon_0 \varepsilon_r S K}{d^2 - x^2} x. \tag{4}$$

By solving formula (4), and considering the boundary condition $x \leq d$, there is

$$
\begin{cases}
x = -\dfrac{\varepsilon_0 \varepsilon_r SK}{V_D} + \sqrt{\left(\dfrac{\varepsilon_0 \varepsilon_r SK}{V_D}\right)^2 + d^2}, & V_D > 0, \\[4mm]
x = -\dfrac{\varepsilon_0 \varepsilon_r SK}{V_D} - \sqrt{\left(\dfrac{\varepsilon_0 \varepsilon_r SK}{V_D}\right)^2 + d^2}, & V_D < 0, \\[4mm]
\qquad\qquad x = 0, V_D = 0.
\end{cases}
\tag{5}
$$

When the TM is near the center of the electrode pair, which is $x \ll d$, formula (4) can be written as

$$
V_{D\text{linear}} = F_{\text{linear}}(x) = \frac{2\varepsilon_0 \varepsilon_r SK}{d^2} x.
\tag{6}
$$

This is a linear function, our purpose is to establish a inverse function so that the position x and the detection voltage V_D satisfy the formula (6) when the TM is far from the center. Combining formulas (5) and (6), the inverse function can be obtained as

$$
V_{D\text{linear}} = f(V_D).
\tag{7}
$$

In formula (7), all the parameters are constant expect V_D, this is a function for the linearization of detection voltage V_D.

The second nonlinear module is H in the blue box. This is the transfer function from driving voltage V_f to electrostatic force F_e, it can be written as[12]

$$
\begin{aligned}
F_e &= H(V_f, x) \\
&= 2\varepsilon_r \varepsilon_0 S \frac{V_p V_f x^2 + (V_p^2 + V_f^2 + V_d^2)dx + V_p V_f d^2}{(d^2 - x^2)^2}.
\end{aligned}
\tag{8}
$$

When the TM is near the center of the electrode pair, which is $x \leq d$, formula (8) can be consider as a linear function.

$$
F_e = H_{\text{linear}}(V_{\text{fc}}) = \frac{2\varepsilon_0 \varepsilon_r S}{d^2} V_p V_{\text{fc}} K_{\text{amp}}.
\tag{9}
$$

In order to establish an inverse function between V_{fc} and V_f, the driving voltage V_{fc} and the electrostatic force F_e are linear. Combining formulas (8) and (9), the inverse function can be obtained as

$$
\begin{aligned}
V_f &= h(V_{\text{fc}}) \\
&= \frac{-(x^2 + d^2)V_p + \sqrt{(x^2 + d^2)^2 V_p^2 - 4x^2 d^2(V_p^2 + V_d^2) - 4\frac{x}{d}V p V_{\text{fc}}(d^2 - x^2)^2}}{2xdK_{\text{amp}}}.
\end{aligned}
\tag{10}
$$

In formula (10), all the parameters are constant expect V_{fc}, this is a function for the linearization of driving voltage V_{fc}. The entire linearization process is described in Fig. 5.
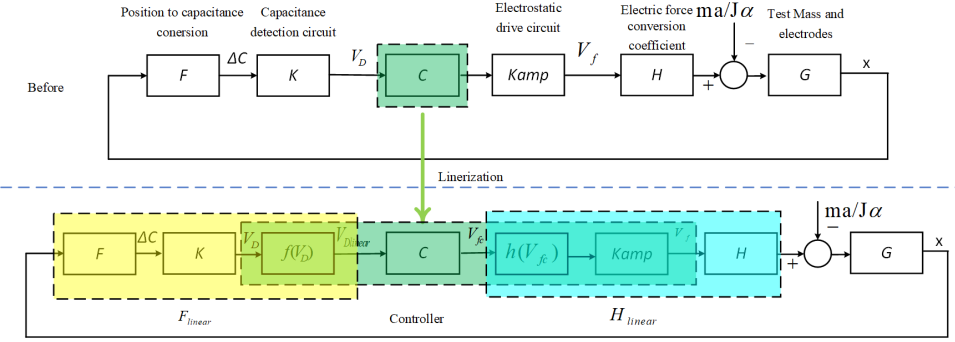
Fig. 5.   Comparison of the ESCS model before and after linearization.

As is shown in Fig. 5, the linearization process and controller are realized in the green box. After linearization, the ESCS consists of F_{linear}, H_{linear}, controller C and kinetic model G, which is a linear system. The kinetic model is a classic spring-like oscillator system, therefore, the kinetic model G can be written as

$$m\ddot{x} = F_{\text{in}} - F_e$$

$$= F_{\text{in}} - 2\varepsilon_r \varepsilon_0 S \frac{(V_p^2 + V_f^2)}{d^3} x - 2\varepsilon_r \varepsilon_0 S \frac{V_p V_f}{d^2}$$

$$= F_{\text{in}} - K_{\text{amp}} \frac{2\varepsilon_0 \varepsilon_r S}{d^2} V_p V_{\text{fc}}, \tag{11}$$

where F_{in} represents external interference into the IS, m is the quality of the TM. From V_{fc} to V_f, the influence of x term is compensated by V_{fc}. The negative electrostatic stiffness is eliminated. The Laplace transform of formula (11) provides the transfer function of the kinetic model of G

$$X(s) = \frac{F_{\text{in}} - K_{\text{driving}} V_{\text{fc}}}{ms^2}, \tag{12}$$

where $K_{\text{driving}} = K_{\text{amp}} \frac{2\varepsilon_r \varepsilon_0 S V_p}{d^2}$ is the gain in the driving system. When the transfer function of the controller $C(s)$ and the electrostatic driving system $G(s)$ is obtained, the closed-loop control system model of the ECSC can be expressed as follows:

$$G(s)_{\text{close}} = \frac{K_{\text{sensor}} G(s) C(s)}{1 + K_{\text{sensor}} G(s) C(s)}, \tag{13}$$

where $G(s) = \frac{K_{\text{driving}}}{ms^2}$ is the transfer function of kinetic model after linearization and $K_{\text{sensor}} = \frac{2\varepsilon_0 \varepsilon_r SK}{d^2}$ is the gain of the capacitance detection module after linearization. $C(s)$ is the transfer function of controller with linearization function formulas (7) and (10). In formula (13), the negative electrostatic stiffness is compensated by formula (10), the system is stable although the TM is not in the center of the electrode pairs and the system can be considered as a linear system in full scale. Then, the controller $C(s)$ will be designed with linear method in following section, and the stability can be guaranteed in large scale.

3. Design of Adaptive Preload Controller

The controller is a core component of the IS, the accuracy and stability of the controller will directly affect the final performance of the IS. Since the IS achieves acceleration measurement through electrostatic forces, the disturbance from electric field is one of the main factors. As we know, a larger prevoltage will cause a larger electrostatic disturbance, we hope that the preload voltage is as small as possible. However, the spacecraft will also suffer a number of unpredictable micrometeoroid strikes, which will cause significant motion and vibration of the spacecraft. These disturbance forces are as large as 10,000 times the nominal acceleration environment. Contrary to the above small preload voltage requirement, we must enhance the preload voltage to compensate these disturbance forces with formulas (8) and (9). To solve this contradiction, the APC is proposed in this paper, the system can automatically change the preload voltage according to the magnitude of overload. In this way, it can not only ensure that the system has a high overload capacity, but also improve the system performance under low overload condition.

First, we estimate a preload voltage range based on the space working environment, defined as $V_{\min}$ and $V_{\max}$, $V_p \in [V_{\min}, V_{\max}]$, $V_p = V_{\min}$ for the initial condition. The environmental acceleration can be measured in real time by formula (9), and $V_p V_{\mathrm{fc}}$ can present the magnitude of environmental acceleration. Then, we choose the comparison of $V_p V_{\mathrm{fc}}$ and V_p^2 as the basis for the change of preload voltage. The adaptive preload law f_{preload} is given as follows:

$$
\begin{aligned}
V_{p\text{-new}} &= f_{\mathrm{preload}}(a, b, c, V_{\mathrm{fc}}) \\
&= \begin{cases}
\text{if} \quad V_p|V_{\mathrm{fc}}| \geq a V_p^2 \text{ then } V_{p\text{-new}} = |V_{\mathrm{fc}}|/b, \\
\text{if} \quad V_p|V_{\mathrm{fc}}| < c V_p^2 \text{ then } V_{p\text{-new}} = b V_p, \\
\text{if} \quad V_{p\text{-new}} > V_{\max} \text{ then } V_{p\text{-new}} = V_{\max}, \\
\text{if} \quad V_{p\text{-new}} < V_{\min} \text{ then } V_{p\text{-new}} = V_{\min}, \\
0 < b \leq a < 1, 0 < c < ab,
\end{cases}
\end{aligned} \tag{14}
$$

where a, b and c are the parameters of adaptive control law. As we can see in formulas (10) and (12), the inverse function for linearization and the gain in the driving system will change with the preload voltage. Generally, the controller $C(s)$ is PID controller with fixed parameters. The transfer function can be written as follows:

$$
C(s) = k_p + \frac{k_i}{s} + k_d s, \tag{15}
$$

where k_p, k_i and k_d are the proportional, integral and differential coefficients of the PID controller, respectively. When the preload voltage is changed, the performance of fixed-parameters PID cannot be guaranteed, it may even cause system work unstable. To solve this problem, an adaptive PID law is derived in this paper.

First, taking formula (15) into formula (13), the closed-loop transfer function can be written as follows:

$$
\begin{aligned}
G(s)_{\text{close}} \\
= \frac{K_{\text{sensor}}K_{\text{driving}}k_d s^2 + K_{\text{sensor}}K_{\text{driving}}k_p s + K_{\text{sensor}}K_{\text{driving}}k_i}{m s^3 + K_{\text{sensor}}K_{\text{driving}}k_d s^2 + K_{\text{sensor}}K_{\text{driving}}k_p s + K_{\text{sensor}}K_{\text{driving}}k_i}.
\end{aligned}
\tag{16}
$$

The closed-loop system characteristic equation can be written as

$$
s^3 + \frac{K_{\text{sensor}}K_{\text{driving}}k_d}{m}s^2 + \frac{K_{\text{sensor}}K_{\text{driving}}k_p}{m}s + \frac{K_{\text{sensor}}K_{\text{driving}}k_i}{m} = 0.
\tag{17}
$$

The characteristic equation can be rewritten as follows:

$$
(s + \beta)(s^2 + 2\varepsilon\omega_n s + \omega_n^2)
$$
$$
= s^3 + (2\varepsilon\omega_n + \beta)s^2 + (2\varepsilon\omega_n\beta + \omega_n^2)s + \beta\omega_n^2 = 0,
\tag{18}
$$

where β is a characteristic root and needs to be greater than zero to ensure system stability, ω_n is the natural angular frequency of the system and ε is the damping ratio of the system. The performance of ESCS can be designed by adjusting these parameters. Combining formulas (17) and (18), the parameters of PID can be written as

$$
f_{\text{PID}}(V_p) = \begin{cases} k_p = \dfrac{m(2\varepsilon\omega_n\beta + \omega_n^2)}{K_{\text{sensor}}K_{\text{driving}}(V_p)}, \\[2mm] k_i = \dfrac{m\omega_n^2\beta}{K_{\text{sensor}}K_{\text{driving}}(V_p)}, \\[2mm] k_d = \dfrac{m(2\varepsilon\omega_n + \beta)}{K_{\text{sensor}}K_{\text{driving}}(V_p)}, \end{cases}
\tag{19}
$$

where β, ω_n and ε are given in advance, m and K_{sensor} are constants which can be measured offline. The gain of driving system $K_{\text{driving}}(V_p)$ is changed with the preload voltage V_p. With formulas (14) and (19), the preload voltage and the parameters of PID can be adjusted online in real time. The control diagram is described in Fig. 6, the green box is the APC.

According to Routh stability criterion, the controller parameters meet the following condition, the control system is stable:

$$
\frac{K_{\text{sensor}}K_{\text{driving}}}{m} > \frac{k_i}{k_p k_d}.
\tag{20}
$$

This is a necessary condition for system stabilization, it reflects the relationship between sensor geometric parameters, electrical parameters and PID parameters, provides a theoretical basis for controller design. With this control method, the control performance under disturbance conditions can be guaranteed to be consistent with that under normal conditions.
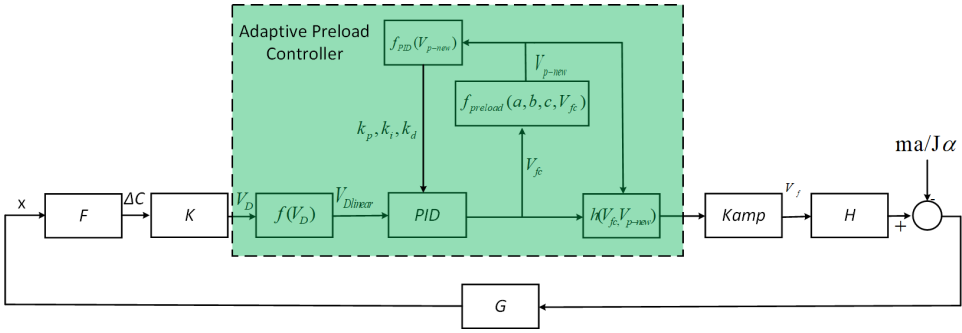
Fig. 6.   Block diagram of APC method.

Table 1.   Structure parameters of the sensor.

	X1	X2	X3	Y	Z1	Z2
Mass m (g)	70.4					
Size (mm)	$40 \times 40 \times 10$					
Electrode Area S (mm^2)	498	249		199	99	
Average gap d (μm)	60			75		

4. Simulation and Analysis

Based on the working principle of the IS, the TM adopts a flat cube structure, the basic parameters of the sensitive structure of the IS are shown in Table 1.

According to formula (9), the max acceleration is determined by the preload voltage V_p, when the feedback voltage is equal to preload voltage, it represents the max acceleration that can be measured. In a 500 km orbit, the GRACE satellite gives a maximum and minimum acceleration disturbance of about 5×10^{-5} and 5×10^{-8} m/s^2, respectively.[18] With the parameters in Table 1, the preload voltage should be larger than 2.5 V to meet the maximum requirement, and a 1.5 V preload voltage will meet the requirement of normal condition. Finally, in order to reserve some margin, a range of preload voltage from 1 V to 5 V is selected for the APC, that is $V_{\min}$=1 V, $V_{\max} = 5$V. In the initial situation, V_p is equal to $V_{\min}$.

The acceleration measurement frequency band is from 0.1 mHz to 1 Hz. Hence, the selection of PID parameters should ensure that the closed-loop bandwidth of the system is larger than 1 Hz, and away from the system resonance frequency (approximately 2.5 Hz). The PID parameters can be selected to obtain resonance frequency around 20 Hz, the natural angular frequency ω_n is $20 \times 2\pi$, the damping ratio ε is 0.707, and a characteristic root β is 100. Then, the parameters of control model are given in Table 2.

The PID parameters can satisfy the stability criterion formula (20). Taking the X1 axis as an example, The actual closed-loop transfer function of the X1 axis is obtained, as shown in formula (21). The closed-loop frequency response curves of the X1 axis are also obtained (Fig. 7).

Table 2.   The initial parameters of control model and PID controller.

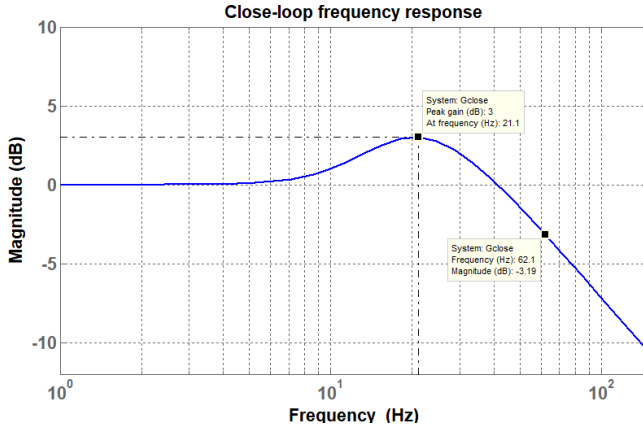|	X1	X2	X3	Y	Z1	Z2
K	1.6×10^{11}	3.2×10^{11}		3.7×10^{11}	7.4×10^{11}	
K_{amp}	5					
K_{driving}	1.23×10^{-5}	6.13×10^{-6}		3.14×10^{-6}	1.57×10^{-6}	
K_{sensing}	4×10^{5}			2.3×10^{5}		
k_p	241			3246		
k_i	1.13×10^{4}			1.53×10^{5}		
k_d	1.99			26.86		

Fig. 7.   Curve of close-loop frequency response.

$$G_{\text{close}} = \frac{9.775s^2 + 1181s + 5.56\times10^4}{0.0352s^3 + 9.775s^2 + 1181s + 5.56\times10^4}. \tag{21}$$

Based on the definition of -3 dB bandwidth, the upper limit of the measurement band of the X1 axis is about 60 Hz, the resonance frequency is the same as designed 21 Hz. The value can meet the requirements of the 1 Hz measurement band specified by the technical requirements.

To verify the effectiveness of APC, a disturbance data is applied to the simulation system, which was collected from our previous experiment,[17] the parameters of APC are $a = b = 0.8, c = 0.4$. The simulation model is established with Simulink tools, the simulation result is shown in Fig. 8.

The preload voltage and PID parameters change with the magnitudes of disturbance. The performance of the ESCS is consistent as expected. The response of the APC can quickly change according to the intensity of the external disturbance. Under the premise that the control system is stable, the preload voltage is optimized and the control efficiency is improved. Compared with the traditional fixed preload method, the system is unstable when the disturbance is too large. The adaptive preload voltage method shows that the stability is significantly improved and the control performance is optimized.
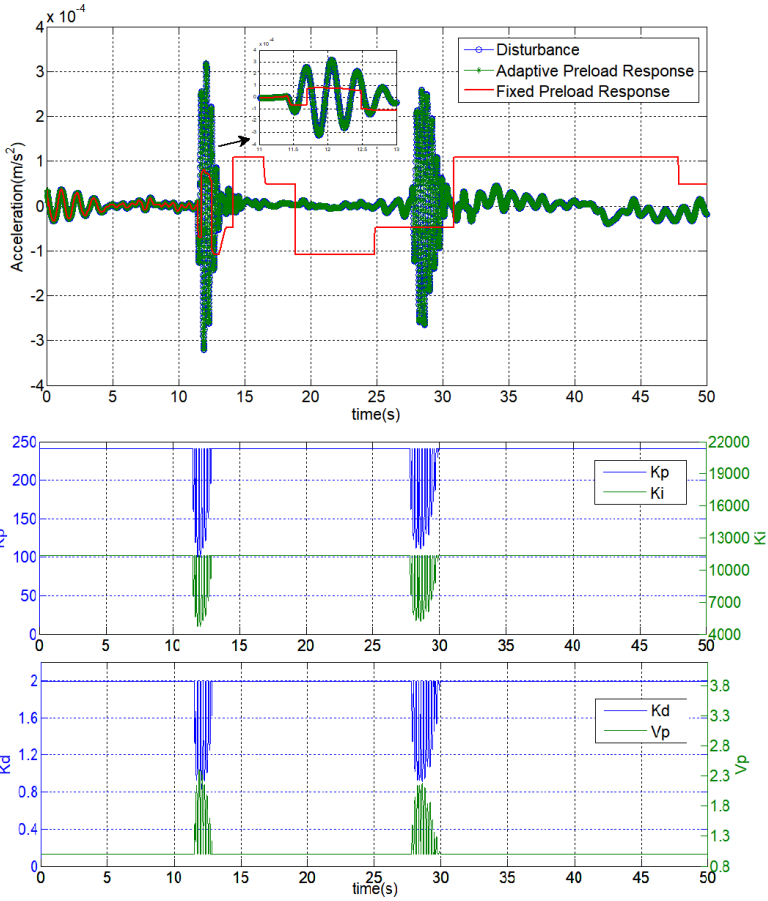
Fig. 8.   Results of close-loop control response with different magnitudes of disturbance.

5. Conclusion and Outlook

In this paper, the working principle, control system model and its linearization are provided. Then, an adaptive preload voltage method is given for ESCS, the stability criterion of the controller is derived. Finally, the simulation and analysis of the adaptive preload voltage are conducted, which give a whole process of the APC design, the performance of the ESCS can meet the requirement as designed. The simulation results show that under different disturbance conditions, the max acceleration disturbance changes from $5 \times 10^{-6} \mathrm{m/s^2}$ to $4 \times 10^{-4} \mathrm{m/s^2}$, not only the preload voltage can adjust with the changing conditions, but also the parameters of PID are optimized accordingly, the ESCS can keep stable at any conditions. Compared with the traditional fixed preload method, we can see that our method has significantly improved the stability margin and the control performance can be guaranteed.

This work proposes a reasonable and feasible method to ensure the stability of the IS in orbit for the future Taiji Program. This work also provides clear ideas for the optimization design of the ESCS and lays a solid foundation for the implementation of the future Taiji Program. Simultaneously, a considerable amount of research and experimental verification work must be conducted on the ground before launching into the space, such as torsion pendulum experiment platform or high voltage suspension experiment platform.

Acknowledgment

References

1. B. P. Abbott *et al.*, *Phys. Rev. Lett.* **6**, 116 (2016).
2. H. Wang, *Chin. J. Space Sci.* **1**, 38 (2018).
3. S. L. Danilishin, E. Knyazev, N. V. Voronchev *et al.*, *Light: Sci. Appl.* **11**, 7 (2018).
4. M. Korobko, Y. Ma, Y. Chen *et al.*, *Light: Sci. Appl.* **8**, 118 (2019).
5. M. Armano, H. Audley, J. Baird, P. Binetruy, M. Born, D. Bortoluzzi, E. Castelli, A. Cavalleri, A. Cesarini, A. M. Cruise *et al.*, *Phys. Rev. Lett.* **6**, 120 (2018).
6. M. Armano, H. Audley, G. Auger *et al.*, *Phys. Rev. Lett.* **23**, 116 (2016).
7. H. B. Tu, Y. Z. Bai, Z. B. Zhou and J. Luo, *J. Phys.: Conf. Ser.* **154**, 012036 (2009).
8. W. Tian, S. C. Wu, Z. B. Zhou, S. B. Qu, Y. Z. Bai and J. Luo, *Rev. Sci. Instrum.* **9**, 83 (2012).
9. Y.-Z. Bai, Z.-B. Zhou, H.-B. Tu, S.-C. Wu, L. Cai, L. Liu and J. Luo, *Phys. China* **2**, 4 (2009).
10. S. Gao, Y. Wang and Y. Li, *Vacuum Cryogen.* **5**, 23 (2017).
11. X. Zhang, C. Li, Z. Wang and J. Min, *Space Electron. Technol.* **1**, 1 (2018).
12. Y. Wang, K. Qi, S. Wang *et al.*, *IEEE Access* **8**, 1 (2020).
13. D. Cyranoski, *Nature* **531**, 10 (2016).
14. H.-S. Liu, Y.-H. Dong, R.-H. Gao, Z.-R. Luo and G. Jin, *Opt. Eng.* **5**, 57 (2018).
15. Q. Xiao, S. Y. Li and W. Y. Chen, *Mach. Electron.* **8**, 15 (2013).
16. S. Yan, K. Zhang, F. Qian, T. Xi and S. Zhang, *Control Eng. China* **17**, 6 (2010).
17. D. Fan, M. Liu, Y. Liu, C. Zhao and J. Dong, Servo loop design of capacitive MEMS accelerometer under high preload voltage, in *Chinese Control and Decision Conf.*, Mianyang, Sichuan, China, 2011, pp. 1341–1344.
18. B. Frommknecht, Integrated sensor analysis of the GRACE mission, Ph D. dissertation, Faculty of Civil Engineering and Surveying, Technical University of Munich, Mnchen, Germany (2007).